Effects of shot peening on fatigue crack initiation and propagation performance of aeronautical materials

Yukui Gao
School of Aerospace Engineering and Applied Mechanics, Tongji University, No. 100 of Zhangwu Road, Yangpu Dist., Shanghai 200092, China, email: yukuigao@tongji.edu.cn

Keywords: shot peening; fatigue; surface integrity; residual stress; crack initiation; crack propagation

Nomenclature

a = crack depth, the dimension size in the z-coordinate direction
R=stress ratio
$R_{p0.2}$=0.2 offset yield strength (MPa)
σ_{ws}=surface fatigue strength/limit (MPa)
R_m=tensile strength (MPa)
σ_{app} =apparent/ normal fatigue strength/limit (MPa)
σ_{loc}=local fatigue strength/limit (MPa)
σ_{locapp}=local applied stress (MPa)
σ_{locrs}=local residual stress (MPa)
σ_{max}=maximum applied stress (MPa)
σ_{mcrs}=the maximum compressive residual stress (MPa)
σ_{mtrs}=the maximum tensile residual stress
c = crack length, the dimension size in the x-coordinate direction
(MPa)
σ_{srs}=surface residual stress (MPa)
σ_{wss} =sub-surface fatigue strength/limit (MPa)
σ_y=yield strength (MPa)
Z_{mcrs}=distance from surface, to the location of maximum compressive residual stress (μm)
Z_0 =depth of compressive residual stress field (μm)
Z_{mtrs}=distance from surface to the location of maximum tensile residual stress (μm)
Δσ=applied stress range (MP

Introduction

Many high strength or ultrahigh strength metallic materials are used in the aircraft industry to manufacture the main components, such as landing gears, wings or engine parts including engine disc or blades. For these metallic alloys, the fatigue properties are affected mainly by surface treatments. To improve the fatigue properties, surface enhancement processes are applied to modify the surface integrity. Surface integrity is a comprehensive concept and it includes many aspects of surface. In the views of fatigue property, the main parameters of surface integrity are residual stresses in surface layer, surface roughness and microstructure [1]. The structural integrity is mainly determined by surface integrity because many fractures occur at surfaces, especially at some defects.

Objectives

There are many investigations on new surface enhancement processes and the effects of surface enhancement on fatigue properties, but less studies on how to quantitatively analyze the effects of residual stresses caused by surface enhancements. Therefore, it is necessary and important to quantitatively determine the effects of surface enhancements for designing components with surface-enhanced layers.

Methodology

High or ultrahigh strength steels, aluminum alloys and titanium alloys were used and their tensile properties are listed in Table 1. Shot peening was used as surface enhancement for the modification of the alloys shown in Table 1, the parameters of this process are also shown in Table 1. Laser shock peening parameters were laser pulse energy density of 2×10^9 W/cm^2, pulse duration of 50 ns, pulse energy of 50 J, at a frequency of 0.54 Hz, with the Almen intensity of 0.08 mm in a C type strip. The residual stresses were measured by X3000 type, Proto LXRD type and μ-X360s type X-ray diffraction stress testers to compare the results by an x-ray diffraction method. With a step-by-step electro-polishing method and the typical profile of residual stress along the depth induced by shot peening or laser shock peening was obtained. The characteristic parameters of residual stress fields for these high-strength metallic materials are listed in Table 2. These characteristics are critical parameters to quantitatively analyze the effects of surface enhancement processes [3,4].

Before and after shot peening, the rotating bending fatigue tests (R=-1) were conducted for the investigated alloys with the exception of 30CrMnSiNi2A steel for which three-point bending fatigue tests (R=0.1) were performed at room conditions.

Results and Analysis

Fatigue crack initiation and fatigue strength/fatigue limit

After surface enhancement, a total of 20 specimens were tested as a group to determine the fatigue strengths/limits for each alloy at 1×10^7 cycles by a staircase method [5,6]. The experimental results are shown in Table 3. Moreover, the effect of surface enhancement is illustrated in the fatigue strengths/limits increscent of surface-enhanced specimens compared with the specimens without surface-enhanced layer by σ_{wss}/σ_{ws} which is also given in Table 3.

Table 1 Tensile property of metallic alloys and the parameters of shot peening [3]

Material	Yield strength ($R_{p0.2}/MPa$)	Tensile strength (R_m/MPa)	Shot	Intensity(mm)	Coverage (%)
40CrNi2Si2MoVA	1643	1950	S330	0.40	100
16Co14Ni10Cr2Mo	1482	1620	S330	0.30	100
30CrMnSiNi2A	1141	1653	S330	0.30	100
0Cr13Ni8Mo2Al	1432	1484	BZ15	0.15	100
2124-T851	400	440	S110	0.25	200
7475-T7351	450	528	S110	0.20	200
7050-T7451	470	539	S110	0.20	200
TC21	1003	1103	BZ20	0.15	200
Ti60	960	1025	BZ20	0.15	200

Table 2 Characteristic parameters of residual stress fields for high-strength materials induced by shot or laser peening [3].

Material	σ_{srs} (MPa)	σ_{mcrs} (MPa)	σ_{mtrs} (MPa)	Z_{mcrs} (μm)	Z_0 (μm)	Z_{mtrs} (μm)
40CrNi2Si2MoVA	-825	-1500	327	40	280	315
16Co14Ni10Cr2Mo	-880	-1000	204	80	300	348
30CrMnSiNi2A	-840	-1150	304	75	450	508
0Cr13Ni8Mo2Al	-883	-1180	148	35	125	214
2124-T851	-210	-275	90	42	260	308
7475-T7351	-308	-380	73	45	300	370
7050-T7451 shot peening	-225	-378	58	100	280	304
Laser peening	-350	-350		0	1800	
TC21	-420	-618	134	60	220	262
Ti60	-450	-646	158	50	220	243

Table 3 Fatigue strengths/limits of smooth specimens of high-strength structural materials [2]

Material	Surface condition	σ_{app} (MPa)	σ_{loc} (MPa)	σ_{sur} (MPa)	σ_{int} (MPa)	Increscent
40CrNi2Si2MoVA	Machining	718	750	750	1065	1.42
	Shot peening	1040	1065			
16Co14Ni10Cr2Mo	Machining	720	720	720	966	1.34
	Shot peening	835	966			
30CrMnSiNi2A	Machining	763	738	738	997	1.35
	Shot peening	887	997			
0Cr13Ni8Mo2Al	Machining	550	580	580	783	1.35
	Shot peening	720	783			
2124-T851	Machining	160	160	160	224	1.40
	Shot peening	206	224			
7475-T7351	Machining	185	185	185	261	1.41
	Shot peening	223	252			
7050-T7451	Machining	263	261	185	206	1.37
	Shot peening	170	150			
TC21	Machining	160	560	400	560	1.40
	Shot peening	206	430			
Ti60	Machining	416	430	430	594	1.38
	Shot peening	580	580			

The fatigue sources always locate at the surface for un-surface-strengthened specimens, whereas for those surface-enhanced specimens, they are located beneath the surface-enhanced layer where the tensile residual stress is [7-9]. When the fatigue source is naturally located at the surface, the local surface stress is called as surface fatigue strength/limit; whereas for those surface-enhanced specimens, when the fatigue source is naturally located at the subsurface or sometimes interior beneath the surface-enhanced layer, therefore, the local fatigue source stress is called as subsurface or internal fatigue strength/limit [10-12].
The dominant process during fatigue source evolution is to form “cyclic meso-yielding areas”. The higher the applied stress is, the larger the formed “cyclic meso-yielding areas”, the higher the probability for initiation and propagation of fatigue cracks and the shorter the life of fatigue source formation will be. The essential processes for meso-yielding and that for yielding in common sense (macro-yielding) are similar, then, the fatigue strength/limit of a metal σ_w should have relation with its yielding strength σ_y and can be analyzed according to the considerations similar to the concept proposed by Hall and Petch [13] for yielding in common sense. Accordingly, σ_w should vary with grain size according to:

$$\sigma_w = \sigma_0 + k_w d^{-1/2} \quad (1)$$

where σ_0 is the stress impeding the dislocation motion along the slip plane within weak grains; k_w is a coefficient reflecting the resistance to cause the dislocation motion “spread across” the grain boundary into the adjacent grains and *d* is the average grain diameter.
But actually, σ_w is much lower than σ_y. According to my consideration, it is because that the dislocation motion in subsurface or internal grains is restricted by the neighboring grains from different sides, while that in the surface grains is only restricted from the internal side and is free from its surface side. Then, k_w , as well as σ_w should be higher for a weak grain located in the interior than that for a weak grain at or near the surface [14].
The improvement of apparent fatigue limit after shot peening should be related to the transfer of fatigue crack source from the surface to the interior. The actual critical stress for fatigue crack source formation in the interior, σ_{wi}, or “internal fatigue limit” is very different from actual critical stress for fatigue crack source formation at the surface, σ_{ws}, or “surface fatigue limit.” The σ_{wi} can be calculated according to the following critical condition:

$$\sigma_{wi} = \sigma_{pi} + \sigma_{ri} \quad (2)$$

where σ_{pi} is the local applied stress of specimen at the position of fatigue crack source (0.23 mm from the surface) when the nominal surface stress is equal to the apparent fatigue limit (1490 MPa) of shot-peened specimen. σ_{pi} can be easily determined according to the elastic mechanics law and its value is equal to 1467 MPa for specimens used in this experiment. σ_{ri} is the local (tensile) residual stress at the position of fatigue crack source.
According to the generally accepted concept, the improvement of apparent fatigue limit of shot-peened metallic parts is directly attributed to the decrease of mean stress of the applied stress cycle due to the induced compressive residual stress. Actually, the latter mechanism should be effective when the surface layer has not been hardened enough during shot peening and the fatigue crack source of specimen still locates at the surface. In this case, the apparent fatigue limit should be related to the surface fatigue limit of metal as well as the compressive

residual stress in the surface layer.

Fatigue life prediction

The main objectives of this part are to investigate the effect of shot peening on small crack growth behavior, to develop methods for quantifying the effects of shot peening-induced residual stresses on small cracks, and also to explore the possibility of applying a total fatigue life prediction methodology based on small crack theory to problems where residual stresses are involved [15].

Compressive residual stress field

The CRSF introduced by shot peening is dependent on both the mechanical properties of target and peening regime. Its characteristic values can be shown as follows [2]:

$$\sigma_{mcrs} = 0.86\sigma_{0.2} - 51 \quad (3)$$

$$\sigma_{srs} = R(114 + 0.563\sigma_{0.2})\ (R = 0.997\sim 1.13) \quad (4)$$

Where R is a coefficient and its value is from 0.997 to 1.13.

$$Z_0 = (1.41D_d - 0.09S)[1 + 0.09(C-1)^{0.55}] \quad (5)$$

$$Z_m \approx 0.28Z_0 \quad (6)$$

The crack "initiation life" for specimens is only a very small part of the total fatigue life. These data provide important experimental support for the use of a total fatigue life approach based on small crack growth analysis.

The calculation of stress intensity factor

The SIF is determined by quadrature of the product of the "crack line stress"σ(X), the stress at the prospective crack site in the crack-free body, and the weight function m(A, X) [9]:

$$K = \int_0^A m(A,X)\sigma(X)dX \quad (7)$$

where A and X are the crack length and the coordinate along the crack, respectively. For convenience, we introduce the dimensionless quantities σ(X)/σ and a = A/W, x=X/W, where σ is a scaling factor with the dimension stress and W is a characteristic length parameter, which is defined for each cracked body. Here we let W = r, the notch radius of the SENT specimens. Eq. (5) therefore has the form:

$$K = f\sigma\sqrt{\pi A} \quad (8)$$

$$f = \int_0^a \frac{\sigma(x)}{\sigma}\frac{m(a,x)}{\sqrt{\pi a}}dx \quad (9)$$

$$x = X/r,\ a = A/r \quad (10)$$

The weight function m(a, x) is related to the crack face displacement by:

$$m(a,x) = \frac{E'}{f_r(a)}\frac{1}{\sigma\sqrt{\pi a}}\frac{\partial u_r(a,x)}{\partial a} \quad (11)$$

where $E' = E$ (plane stress) or $E' = E/(1-v^2)$ (plane strain), where E is the Young's modulus and v is the Poisson ratio, and f_r and u_r are the SIF and the dimensionless crack displacement ($u_r(a,x) = U_r(a,x)/W$) for the reference load case σ(x), respectively. The dimensionless crack displacement is usually given as:

$$u_r(a,x) = \frac{U_r(a,x)}{W} \tag{12}$$

Fatigue crack closure

Small crack growth rates and fatigue lives of naturally occurring small cracks in shot peened and un-peened specimens were calculated using small crack theory and a crack closure model [16]. The predicted results agree well with the experimental data.

The applied stress intensity factor is:

$$\Delta K = K_{max} - K_{min} \tag{13}$$

Where K_{max} is the maximum stress intensity factor and K_{min} is the minimum stress intensity factor.

$$\frac{da}{dN} = C \cdot \Delta K^m \tag{14}$$

Where a is the length of crack and N is cyclic times while C and m are determined by material itself.

The efficient stress intensity factor is:

$$\Delta K_{eff} = K_{max} - K_{op} \tag{15}$$

Where K_{op} is open stress intensity factor.

So the crack closure coefficient is:

$$\mathrm{U} = \frac{\Delta K_{eff}}{\Delta K} = \frac{K_{max} - K_{op}}{K_{max} - K_{min}} = \frac{P_{max} - P_{op}}{P_{max} - P_{min}} = \frac{1 - \frac{P_{op}}{P_{max}}}{1 - R} \tag{16}$$

Where K_{op} is open stress intensity factor; P_{op} is crack opening loads; P_{max} is the maximum crack opening loads; P_{min} is the minimum crack opening loads.

Then the Paris formula can be modified as follows:

$$\frac{da}{dN} = C \cdot \left(\Delta K_{eff}\right)^m = C \cdot (U \cdot \Delta K)^m \tag{17}$$

Data for the lengths of small cracks as a function of loading cycles were recorded using AC paper replicas. Typical replica images by SEM showing the crack length after different numbers of cycles are shown in Fig. 1 and 2 for un-peened and shot peened specimens, respectively. Compared with un-peened specimens, the small crack growth rates are very much lower for shot peened specimens. The difference increases rapidly with increasing crack length.

Fig. 3 demonstrates that the small cracks are all surface racks and that the crack length in the thickness direction, is similar to the crack length in the width direction, therefore da/dN = dc/dN.

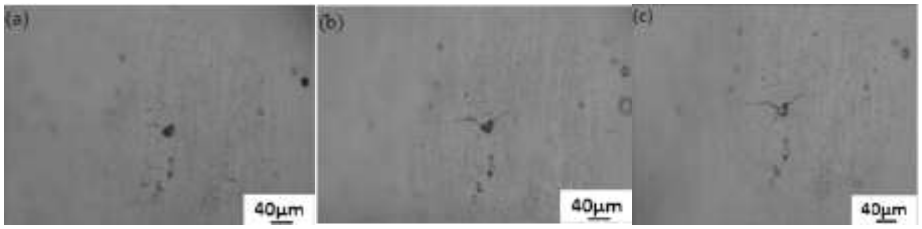

Fig. 1 Replica SEM images showing small crack growth in an un-peened specimen of 7475-T7351 aluminum alloy for N cycles: (a) N = 3000; (b) N = 6000; (c) N = 9000 [4].

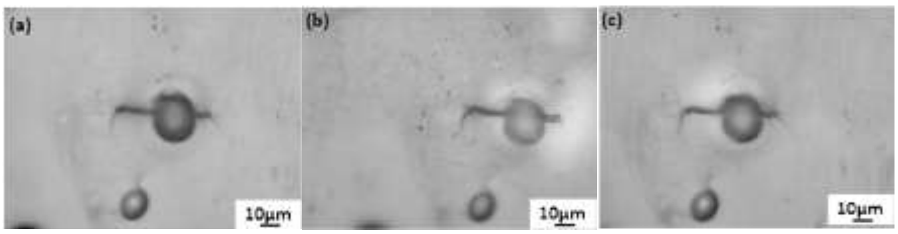

Fig.2 Replicas SEM images showing small crack growth in a shot peened specimen of 7475-T7351 aluminum alloy for N cycles: (a) N = 6000; (b) N = 7000; (c) N = 8000 [4].

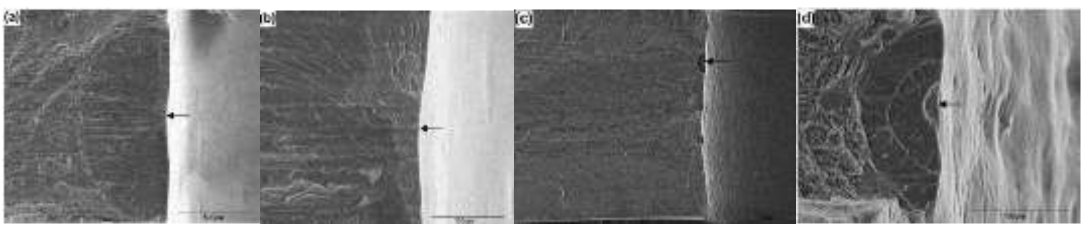

Fig.3 SEM fracture surfaces of (a and b) un-peened and (c and d) shot peened specimens [4].

Conclusions

(1) The electro-polishing has a beneficial effect on the fatigue limit in comparison with that of ground specimen due to the decrease of the surface toughness, but the effect is not notable. Further shot peening induces high compressive residual stress field in the surface layer, transfers the fatigue crack source into the interior and then increases the fatigue limit for about 36%.

(2) By taking the residual stresses into account, total fatigue lives for materials/structures containing residual stresses can be predicted using small crack theory, by use of the crack closure-based fatigue life prediction code FASTRAN.

(3) The fatigue sources always locate at surface for un-surface-strengthened specimens, whereas for those surface-enhanced specimens, they are located beneath the surface-enhanced layer.

References

[1] Gao Y K, Li X B, Yang Q X, et al. Influence of surface integrity on fatigue strength of 40CrNi2Si2MoVA steel[J]. Materials Letters, 2007, 61(2):466-469.

[2] Gao Y. Bending fatigue strengths/limits of smooth specimens with and without surface-enhanced layer of aeronautical metallic alloys[J]. International Journal of Structural Integrity, 2011, 2(3):357-365.

[3] Gao Y K, Wu X R. Experimental investigation and fatigue life prediction for 7475-T7351 aluminum alloy with and without shot peening-induced residual stresses[J]. Acta Materialia, 2011, 59(9):3737-3747.

[4] Padilla H A, Boyce B L. A Review of Fatigue Behavior in Nanocrystalline Metals[J]. Experimental Mechanics, 2010, 50(1):5-23.

[5] Shanyavskiy A, Banov M. The twisting mechanism of subsurface fatigue cracking in Ti–6Al–2Sn–4Zr–2Mo–0.1Si alloy[J]. Engineering Fracture Mechanics, 2010, 77(11):1896-1906.

[6] Shanyavskiy A A, M.D. Banov, Zakharova T P. Principles of physical mesomechanics of nanostructural fatigue of metals. I. Model of subsurface fatigue crack nucleation in VT3-1 titanium alloy[J]. Physical Mesomechanics, 2010, 13(3–4):133-142.

[7] Mano H, Kondo S, Matsumuro A. Microstructured surface layer induced by shot peening and its effect on fatigue strength[J]. Journal of the Japan Institute of Metals, 2006, 70(5):1-4.

[8] Wang S W, Nishida S I, Hattori N, et al. Effect of Plastic Deformation by Roller-Working on Fatigue Strength of Notched Specimen.[J]. Jsme International Journal, 2008, 43(4):415-422.

[9] Tanaka H, Kobayashi T, Nakasato F, et al. Effects of Alloying Elements and Shot Peening on Impact Fatigue Strength of Carburized Steels[J]. Tetsu- to- Hagane, 1993, 79:90-97.

[10] Xiao H, Chen Q, Shao E, et al. The effect of shot peening on rolling contact fatigue behaviour and its crack initiation and propagation in carburized steel[J]. Wear, 1991, 151(1):77-86.

[11] Gao Y K, Yao M, Shao P G, et al. Another mechanism for fatigue strength improvement of metallic parts by shot peening[J]. Journal of Materials Engineering and Performance, 2003, 12(5):507-511.

[12] Liu W, Dong J, Zhang P, et al. Effect of Shot Peening on Surface Characteristics and Fatigue Properties of T5-Treated ZK60 Alloy[J]. Materials Transactions, 2009, 50(4):791-798.

[13] E.O. Hall: Yield Point Phenomena in Metals, Plenum Publishing Company, New York, NY, 1970.

[14] Gao Y K, Lu F, Wu X R, et al. Influence of carburization followed by shot peening on fatigue property of 20CrMnTi steel[J]. Journal of Materials Engineering and Performance, 2005, 14(5):591-595.

[15] Wang R Z, Ru J L, Li X B, et al. A Micro- meso-process Theory of Fatigue Crack Initiation and Theory of Internal Fatigue Limit[J]. Transactions of Metal Heat Treatment, 1995(2):184.

[16] Abe T, Furuya Y, Matsuoka S. Cycle fatigue properties of 1800 MPa-class JIS-SUP7 spring steel. Fatigue Fract Eng Mater Struct[J]. Fatigue & Fracture of Engineering Materials & Structures, 2004, 27(2):159-167.